ORIGINAL PAPER

Theoretical study on the aromaticity from d-AOs in cationic X_3^+ (X = Sc, Y, La) clusters

Xian Xing Chi · Xing Zhan Lin

Abstract The stable structures and aromatic characters for three cationic X_3^+ (X = Sc, Y, and La) and three relevant neutral X_3Cl (X = Sc, Y, La) clusters are investigated at the DFT and post HF level of theory. The calculated results show that the X_3^+ cations each has two stable structures: the regular trigon (D_{3h}) and the line ($D_{\infty h}$) with the regular trigon (D_{3h}) being the ground state, while for three neutral X_3Cl clusters, Sc_3Cl has three stable isomers: the trigon-pyramidal (C_{3v}), bidentate (C_{2v}-1), and C_{2v}-2 structures, Y_3Cl and La_3Cl each has only two stable isomers: the trigon-pyramidal (C_{3v}) and bidentate (C_{2v}-1) structures. The ground states for three X_3Cl species are all the bidentate (C_{2v}-1) isomers. The calculations of the resonance energy (RE) and NICS show that trigonal X_3^+ isomers exhibit higher degree of aromaticity. The detailed molecular orbital analyzes reveal that the isolated trigonal Sc_3^+ and Y_3^+ cations each has one delocalized π-type MO and shows single π-aromaticity, while the isolated trigonal La_3^+ cation has one delocalized σ-type MO and shows single σ-aromaticity. The single π- or σ-aromaticity for X_3^+ are attributed to the contributions mainly from the d AOs of the corresponding transition metal X atoms. However, when a singly negatively charged counterion Cl^- is added to Sc_3^+, Y_3^+, and La_3^+ cations respectively, the aromatic type for the two Sc_3^+, Y_3^+ units in the corresponding neutral Sc_3Cl, Y_3Cl complexes are changed from π-aromaticity into σ-aromaticity, whereas the σ-aromaticity of the La_3^+ units in the La_3Cl complex keeps unchanged in this process. Thus three Sc_3^+, Y_3^+, La_3^+ units in the corresponding X_3Cl complexes all have only one σ-type MO and exhibit single σ-aromaticity.

Introduction

The concept of aromaticity, one of the most significant concepts in chemistry, generally used to describe cyclic, planar, and conjugated molecules with delocalized π-bonds and unusual stability, such as benzene and its derivatives [1, 2]. In recent years the aromatic concept has been successfully extended from traditional organic compounds to pure all-metal clusters [3–12] due to the pioneering works done by Boldyrev's group [3]. Advances in all-metal aromaticity and antiaromaticity have been comprehensively reviewed by Boldyrev and Wang [13]. In addition to the aromaticities for planar, ring-shaped species, the aromaticities in three dimentional (3D)structtures of clusters, including spherical aromaticity of inorganic cage clusters, such as Sn_{12}^{2-} and Pb_{12}^{2-} clusters, have been intensively studied and many important progresses have been made in recent decades [14–20].

For the aromaticity of planar molecules, some generally accepted criteria have been formulated and often used for identifying the aromaticity of molecules, e.g., high energetical stability, cyclic planar geometries, and unusual magnetic properties such as nucleus-independent chemical shift (NICS) proposed by Schleyer et al. [2, 3, 21–30].

From the point of view of molecular orbital (MO) and electronic structure, the type of aromaticity has also been expanded from initially π-aromaticity of benzene to σ-, π-, δ-aromaticity as well as their mixed multiple-fold aroma-

X. X. Chi (✉) · X. Z. Lin
College of Physics & Electronic Information Enginerring,
WenZhou University,
WenZhou 325035, Peoples Republic of China
e-mail: chixx@wzu.edu.cn

ticity for all-metal clusters in the last years [5, 8, 9, 31, 32]. For transition-metal-containing clusters, MO analyzes on their aromaticities were reported recently [12, 33–36]. Tsipis et al. [33] studied a new class of cyclic hydrocoppers Cu_nH_n (n=3-6) using DFT and showed that the cyclic hydrocoppers Cu_nH_n (n=3-6) exhibit stronger aromaticity with a composite bonding mode involving σ, π, and δ components, resulting from the bonding interaction of the 3d atomic orbitals (AOs) of the Cu atoms. Huang et al. [34] reported experimental and theoretical evidence of d-orbital aromaticity in two early 4d and 5d transition metal oxide clusters, namely $M_3O_9^-$ and $M_3O_9^{2-}$ (M = W, Mo). For the Cu_4^{2-} ring there are different viewpoints about the contribution of valence MOs to its aromaticity. Wannere et al. [35] considered that the aromaticity for the Cu_4^{2-} ring mainly arises from the d orbital (and some s) contributions of Cu atom using canonical molecular orbital NICS (CMO-NICS) analyzes. Whereas the experimental and computational studies of M_4Na^- (M = Cu, Au) clusters by Sundholm et al. [12] showed that the Cu_4^{2-} ring is σ aromatic mainly from the 4 s bonding interactions and the d orbitals do not play any significant role for the electron delocalization effects. In a previous paper [37], our theoretical investigation proved that the trigonal Cu_3^+ ring possesses only σ-aromaticity originating from Cu 4 s orbitals in favor of the conclusion made by Sundholm.

Recently we have investigated theoretically a new class of all-metal anionic three-membered clusters X_3^- (X = Sc, Y, and La), which are corroborated to possess doubly aromatic characters (σ and π) originating primarily from d AOs of the transition metal atoms Sc, Y, and La [38]. In the current work, we advance the probing of the aromaticity of three-membered X_3^- clusters to three new cationic X_3^+ (X = Sc, Y, and La) species. Various stable structures and aromatic characters of cationic X_3^+ (X = Sc, Y, and La) as well as the relevant neutral X_3Cl (X = Sc, Y, La) clusters are investigated with ab initio calculations, which can be expected to possess only single π- or σ-aromaticity originating primarily from d AOs of the transition metal atoms Sc, Y, and La. In view of only singlet states for the anionic X_3^- (X = Sc, Y, and La) species being global minima and possessing aromatic characters in our previous studies on X_3^- (X = Sc, Y, and La) species, the current ab initio calculations only involve the singlet states of the cationic X_3^+ (X = Sc, Y, and La) species.

Computational methods

The structural optimizations and vibrational frequency calculations for the all-metal cations X_3^+ and neutral X_3Cl (X = Sc, Y, and La) clusters are carried out using four methods: two density functional theory (DFT) B3LYP, B3PW91 and two

correlated ab initio MP2, CCSD(T). B3LYP is a DFT method using Beck's three parameters functional (B3) [39] along with the Lee, Yang, and Parr correlation functional (LYP) [40]. B3PW91 uses B3 along with Perdew-Wang 1991 correlation functional [41]. MP2 is the second-order Møller-Plesset perturbation theory [42, 43]. CCSD(T) is the coupled-cluster theory using singles and doubles level augmented by a perturbative correction for triple excitations [44–46]. The extended 6-311 + G* basis set is used for Sc, Cl atoms and the LANL2DZ basis set including the effective core potential (ECP) and some relativistic effect is adopted for the heavier metal Y, La atom.

The resonance energy (RE), or aromatic stabilization energy (ASE) [47–53] is an important energetic criterion for the aromaticity. RE (or ASE) is the extra stabilization energy relative to that of a reference structure where resonance is not present. RE has been used quite successfully for a long time in quantifying aromaticity. At present, several calculation schemes to estimate the resonance energies have been used, which depend strongly on the formulation of the given reaction [9, 31, 51, 53].

In order of the reliability of computed RE values, here two often-used schemes for RE calculation are adopted as follows:

One scheme is through Eq. 1 to compute RE (denoted as RE_1, Boldyrev's scheme), analogous to the method suggested by Boldyrev and co-workers in calculating the REs of Li_3^+ [9].

$$X_3Cl\left(C_{2v} - 1, {}^1A_1\right) \rightarrow X_2({}^1\Sigma_g) + XCl({}^1\Sigma)(X = Sc, Y, La)$$
(1)
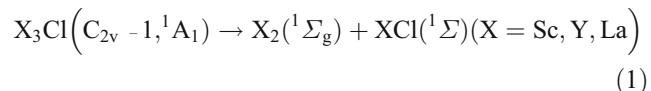
The RE is calculated as the reaction energy of Eq. 1.

Another scheme is Dewar's approach (denoted as RE_2, Dewar's scheme) [2, 51], by which the REs of the trigonal X_3^+ isomers are calculated through Eq. 2,

$$RE(X_3^+) = AE\left(X_3^+(D_{3h}) \rightarrow 2X({}^2D) + X^+\right) - mBE(X_2({}^1\Sigma_g)$$
$$\rightarrow 2X({}^2D))(X = Sc, Y, La),$$
(2)
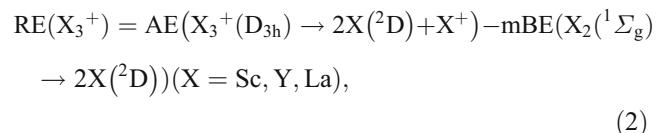
where AE (X_3^+) is the atomization energy of trigonal X_3^+ isomer. BE is the reference bonding energy of a localized X-X single bond, which can be considered as the dissociation energy by the reaction: $X_2({}^1\Sigma_g) \rightarrow 2X({}^2D)$. The factor m before the BE term in the right side of Eq. 2 is the number of bonding electron pairs. Here m=1, due to the presence of only two valence electrons occupying one delocalized bonding π or σ MO in each of trigonal X_3^+ isomers (details of the MO analysis are given in Sect. 3.3

below). The Dewar's scheme had successfully been used to estimate the RE of all-metal Al_4^{2-} cluster by Zhan and co-workers [31].

NICS is the negative isotropic value of the magnetic shielding tensor at or above the geometrical centers of rings or clusters. Aromaticity is characterized by negative NICS value, antiaromaticity by positive NICS value, and nonaromatic compounds by NICS value close to zero. In this study, four NICS values for each trigonal isomer of these X_3^+ clusters are calculated at four positions: the center of the ring and three points 0.5Å, 1.0Å, 1.5Å above the center of the ring. For each of the trigon-pyramidal (C_{3v}) X_3Cl isomers, four NICS values are also calculated at four positions: the center of the trigonal unit X_3^+ in X_3Cl and three points 0.5Å, 1.0Å, 1.5Å above the center of the trigonal unit X_3^+. Four NICS values at four points for each of X_3^+ and X_3Cl are denoted NICS (0.0), NICS (0.5), NICS (1.0), NICS (1.5) respectively.

All calculations in this work are performed using the Gaussian03 program [54]. The MO pictures are drawn using the Gaussiview 3.0 program [55].

Results and discussion

The stable structures for X_3^+ and X_3Cl clusters

Two possible structures (D_{3h} and $D_{\infty h}$) for X_3^+ (X = Sc, Y, and La) cations and three possible structures (C_{3v}, C_{2v}-1, C_{2v}-2) for neutral X_3Cl (X = Sc, Y, La) clusters (Fig. 1) are investigated. The bond lengths R, total electronic energies E_{tot} (including zero-point energies (ZPE)), relative energies E_{re}, number of imaginary frequencies (Nimag), and vibrational frequencies υ_i for two optimized structures (D_{3h} and $D_{\infty h}$) of three X_3^+ species with four methods: B3LYP, B3PW91, MP2, and CCSD(T) are listed in Table 1. For three X_3Cl species, geometrical parameters, E_{tot}, E_{re}, and Nimag for their optimized structures (C_{3v}, C_{2v}-1, C_{2v}-2) using the same four methods are listed in Table 2. The vibrational frequencies υ_i for three optimized structures (C_{3v}, C_{2v}-1, C_{2v}-2) of X_3Cl using the same four methods are listed in Table 3.

The calculated results in Table 1 show that the regular trigonal (D_{3h}) and the linear ($D_{\infty h}$) structures are stable

with no imaginary frequencies to arise using all four methods, except for three cases: the trigonal Sc_3^+ with B3PW91, the linear Sc_3^+ with MP2 and the trigonal La_3^+ with MP2 method, in which there is one imaginary frequency to arise. The trigonal structures (D_{3h}) are energetically lower than the linear ones ($D_{\infty h}$) with all the four methods. The trigonal structures (D_{3h}) are lower in average E_{tot} with three methods (B3LYP, B3PW91, MP2) than the linear ones ($D_{\infty h}$) by 37.4 kcal mol^{-1} for Sc_3^+, 22.9 kcal mol^{-1} for Y_3^+, 16.4 kcal mol^{-1} for La_3^+.

From Table 2 and Table 3, one can see that for Sc_3Cl species, the trigon-pyramidal (C_{3v}), bidentate (C_{2v}-1), and C_{2v}-2 structures (Fig. 1c, d, e) are stable. For the pyramidal (C_{3v}) and C_{2v}-2 structures, the calculated vibrational frequencies are all real using four or three methods. For the bidentate (C_{2v}-1) structure of Sc_3Cl, Nimag=0 with MP2 and CCSD(T) methods, whereas Nimag=1 with the other two methods of B3LYP and B3PW91. In view of MP2 and CCSD(T) methods being more reliable and the E_{tot} of C_{2v}-1 isomer being the lowest in energy among three isomers for Sc_3Cl, the bidentate (C_{2v}-1) structure should be stable and the ground state. For Y_3Cl and La_3Cl species, the trigon-pyramidal (C_{3v}) and bidentate (C_{2v}-1) isomers (Fig. 1c, d) are stable due to their Nimag=0 using all four methods with the bidentate (C_{2v}-1) isomers also being the ground state. The difference in energy between the pyramidal (C_{3v}) and bidentate (C_{2v}-1) isomers is very small. With the best theoretical level of CCSD(T), the bidentate (C_{2v}-1) isomer is lower in energy than the pyramidal one by 8.8 kcal mol^{-1} for Sc_3Cl, 2.5 kcal mol^{-1} for Y_3Cl, and 29.0 kcal mol^{-1} for La_3Cl respectively. Comparison among the geometrical data in Table 1 and Table 2 indicates that the isolated trigonal X_3^+ isomers seem to undergo very little structural changes in forming these stable isomers of the corresponding X_3Cl clusters under the same method and preserve the structural integrity of each X_3^+ unit.

The REs calculated with two schemes described in section 2 for the trigonal X_3^+ clusters are listed in Table 4 using three methods of B3LYP, MP2, CCSD(T). Basis set 6-311 + G* is used for Sc, Cl and LANL2ZD for Y, La. From Table 4 one can see that the calculated RE values for the trigonal X_3^+ isomers are rather large, compared with the

Fig. 1 Possible isomers for X_3^+ and X_3Cl (X = Sc, Y, and La) species
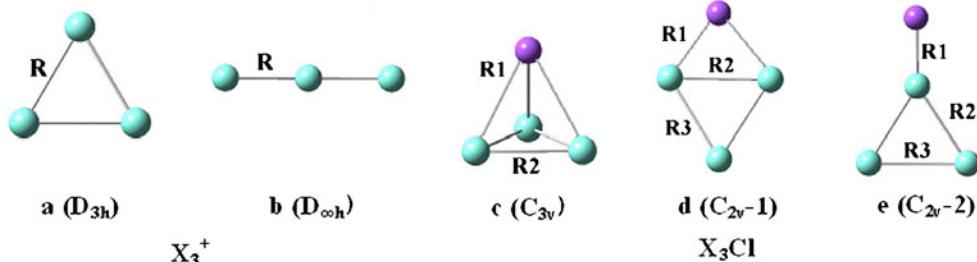
Table 1 The bond lengths R (Å), total electronic energies E_{tot} (including ZPE, hartree), relative energies E_{re} (kcal mol^{-1}), number of imaginary frequencies (Nimag), and vibrational frequencies υ_i (cm^{-1}) of two structures: trigonal (D$_{3h}$) and linear (D$_{\infty h}$) for Sc$_3^+$, Y$_3^+$, and La$_3^+$ species

	Trigonal (D$_{3h}$, ^{1}A$'_1$)					Linear(D$_{\infty h}$, $^1\Sigma_g$)			
	B3LYP	B3PW91	MP2	CCSD(T)		B3LYP	B3PW91	MP2	CCSD(T)
Sc$_3^+$									
R	2.725	2.704	2.991	3.022		2.728	2.727	2.362	—^{a}
E_{tot}	-2281.71687	-2281.53947	-2279.03237	-2279.08803		-2281.68896	-2281.50191	-2278.91892	
E_{re}	0.0	0.0	0.0	0.0		17.5	23.6	71.2	
Nimag	0	1	0	0		0	0	1	
υ_1(a$_1'$)	272	296	252	234	υ_1 (Π_u)	96	100	104	
υ_2(e')	398	i812	271	238	υ_2 (Π_u)	96	100	880	
υ_3(e')	579	220	271	238	υ_3 (Σ_g)	164	167	335	
					υ_4 (Σ_u)	221	232	i162	
Y$_3^+$									
R	3.234	3.214	3.477	3.449		2.966	2.958	3.107	3.226
E_{tot}	-113.47401	-113.54543	-112.56048	-112.59940		-113.43939	-113.50601	-112.52513	-112.56775
E_{re}	0.0	0.0	0.0	0.0		21.7	24.7	22.2	19.9
Nimag	0	0	0	0		0	0	0	0
υ_1(a$_1'$)	189	196	156	159	υ_1 (Π_u)	72	75	62	47
υ_2(e')	103	88	128	115	υ_2 (Π_u)	72	75	62	47
υ_3(e')	103	88	128	115	υ_3 (Σ_g)	120	122	102	92
					υ_4 (Σ_u)	183	192	153	166
La$_3^+$									
R	3.617	3.582	3.907	3.845		3.268	3.241	3.257	4.163^b
E_{tot}	-93.35881	-93.44945	-92.45906	-92.50713		-93.34539	-93.43348	-92.40989	-92.48334^c
E_{re}	0.0	0.0	0.0	0.0		8.4	10.0	30.9	
Nimag	0	0	1	0		0	0	0	
υ_1(a$_1'$)	132	139	i204	104	υ_1 (Π_u)	54	57	28	
υ_2(e')	98	94	1513	103	υ_2 (Π_u)	54	57	239	
υ_3(e')	98	94	1513	103	υ_3 (Σ_g)	86	87	108	
					υ_4 (Σ_u)	124	139	286	

^{a} The solid line denotes the failure both in the structural optimization and frequency calculations

^{b} It denotes success in the structural optimization calculation but failure in the frequency calculation

^{c} It does not include ZPE

REs value of Li$_3^+$ species, which is 35.7 kcal mol^{-1} given by Boldyrev's group [9] with Boldyrev's scheme. The larger RE values show their stronger aromaticities. The RE values given by two schemes under the same method have some differences. The RE values computed with Dewar's scheme are larger than the ones with Boldyrev's scheme. However, the two RE computing schemes give the same aromaticity order: Y$_3^+$, Sc$_3^+$ aromaticities are close and stronger than La$_3^+$ one.

Magnetic characteristics of aromaticity for the trigonal X$_3^+$ cations

The calculated NICS values of the trigonal (D$_{3h}$) X$_3^+$ and the trigon-pyramidal (C$_{3v}$) X$_3$Cl isomers are listed in

Table 5 with method GIAO-HF, GIAO-B3LYP/6-311 + G*//B3LYP/6-311 + G* for Sc$_3^+$ and Sc$_3$Cl, GIAO-HF, GIAO-B3LYP/LANL2DZ//B3LYP/LANL2DZ for Y$_3^+$ and La$_3^+$, and GIAO-HF, GIAO-B3LYP/mixed basis set//B3LYP/mixed basis set for Y$_3$Cl and La$_3$Cl (the mixed basis set: 6-311 + G* for Cl and LANL2DZ for Y, La). For comparison, the similar four NICS values for Mg$_3$Na$^-$ species calculated with GIAO-HF, GIAO-B3LYP/6-311 + G*//B3LYP/6-311 + G* are also listed in Table 5. Comparison among these NICS data in Table 5 indicates that four NICS values of three trigonal X$_3^+$ isomers each are almost negative with NICS (0.0) being the maximum negative one, which show their higher degree of aromaticity, except for the NICS values of the trigonal Sc$_3^+$ isomer with B3LYP method, which are positive, abnormally large

Table 2 The bond lengths R_i (Å), total electronic energies E_{tot} (including ZPE, hartree), relative energies (E_{re}, kcal mol^{-1}), and number of imaginary frequencies (Nimag) of three optimized structures (C_{3v}, C_{2v}-1, and C_{2v}-2) for X_3Cl (X=Sc, Y, La) species

methods	Sc$_3$Cl			Y$_3$Cl			La$_3$Cl		
	C$_{3v}$	C$_{2v}$-1	C$_{2v}$-2	C$_{3v}$	C$_{2v}$-1	C$_{2v}$-2	C$_{3v}$	C$_{2v}$-1	C$_{2v}$-2
B3LYP									
R1	2.649	2.532	2.350	2.869	2.697	2.515	3.019	2.835	2.736
R2	2.830	3..005	2.703	3.193	3.374	3.055	3.490	3.822	3.765
R3		2.703	3.100		3.046	3.447		3.345	3.576
E$_{tot}$	-2742.26116	-2742.27377	-2742.25968	-573.99495	-574.00496	-573.98681	-553.89341	-553.90615	-553.84282
E$_{re}$	0.0	-7.9	0.9	0.0	-6.3	5.1	0.0	-8.0	31.7
Nimag	0	1	0	0	0	1	0	0	2
B3PW91									
R1	2.622	2.515	2.335	2.840	2.677	2.499	2.983	2.810	2.720
R2	2.816	2.986	2.699	3.168	3.357	3.038	3.457	3.785	3.726
R3		2.692	3.090		3.024	3.425		3.319	3.536
E$_{tot}$	-2742.02728	-2742.04127	-2742.02309	-574.01282	-574.02489	-574.00338	-553.93395	-553.94759	-553.87742
E$_{re}$	0.0	-8.8	2.6	0.0	-7.6	5.9	0.0	-8.6	35.5
Nimag	0	1	0	0	0	1	0	0	2
MP2									
R1	2.619	2.485	2.322	2.895	2.696	2.498	3.058	2.831	2.696
R2	2.889	3.093	2.750	3.374	3.481	3.567	3.700	3.953	3.970
R3		2.834	3.190		3.308	3.461		3.504	3.892
E$_{tot}$	-2738.97174	-2738.99674	-2738.97054	-572.49634	-572.50579	-572.48720	-552.40735	-552.42202	-552.36606
E$_{re}$	0.0	-15.7	0.8	0.0	-5.9	5.7	0.0	-9.2	25.9
Nimag	0	0	0	0	0	2	0	0	1
CCSD(T)									
R1	2.651	2.518	—[a]	2.917	2.723	2.503[b]	3.078	2.883	2.697[b]
R2	2.916	3.094		3.400	3.471	3.621	3.709	3.967	4.012
R3		2.844			3.318	3.489		3.516	3.848
E$_{tot}$	-2739.04646	-2739.06051		-572.55237	-572.55628	-572.53886[c]	-552.42037	-552.46662	-552.42946[c]
E$_{re}$	0.0	-8.8		0.0	-2.5		0.0	-29.0	
Nimag	0	0		0	0		0	0	

[a] The solid line denotes the failure both in the structural optimization and frequency calculations

[b] It denotes success in the structural optimization calculation but failure in the frequency calculation

[c] It does not include ZPE

and could be considered to be unreasonable. Three maximum negative NICS (0.0) values under one method for X_3^+ show that La$_3^+$ aromaticity is stronger than Sc$_3^+$ and Y$_3^+$ ones, which are close. Comparison with aromaticity order obtained from RE data in Table 4, the two aromaticity orders for three trigonal Sc$_3^+$ isomers by RE and NICS data respectively have some differences. For X_3Cl, NICS (1.0) and NICS (1.5)) among four NICS values are all negative, with the maximum negative one being NICS (1.5), lying at the point 1.5Å above the center of the trigonal unit X_3^+ in X_3Cl. This shows that addition of a counterion Cl$^-$ to X_3^+ exerts greater influence on NICS values in isolated X_3^+ cations.

Single π- or σ-aromaticity for the trigonal X_3^+ cations

In this section, we will further explore the aromaticity of the trigonal X_3^+ cations through MO analyzes. Three transition metal atoms Sc, Y, and La each has three valence electrons: one d-AO electron and two filled s-AO electrons. Each of X_3^+ species has eight valence electrons and occupied four valence MOs: one HOMO and three energetically lower valence MOs, denoted HOMO-n (n=1-3) respectively. Each of three related neutral X_3Cl species has 16 valence electrons, among which there are eight valence electrons possessed by the monoanionic counterions Cl$^-$ which occupy fully the outermost 2p and

Table 3 Vibrational frequencies (cm^{-1}) of three optimized structures (C$_{3v}$, C$_{2v}$-1, and C$_{2v}$-2) for three X$_3$Cl (X = Sc, Y, La) species

isomers	Sc$_3$Cl				Y$_3$Cl				La$_3$Cl			
	B3LYP	B3PW91	MP2	CCSD(T)	B3LYP	B3PW91	MP2	CCSD(T)	B3LYP	B3PW91	MP2	CCSD(T)
C$_{3v}$(^{1}A$_1$)												
$\nu_{1,2}$(e)	104	119	113	106	54	69	53	48	92	104	103	72
$\nu_{3,4}$(e)	210	217	243	214	141	147	130	123	104	110	144	86
ν_5(a$_1$)	236	243	251	237	178	184	173	155	138	143	114	106
ν_6(a$_1$)	300	308	325	295	221	228	217	211	205	211	195	193
C$_{2v}$-1(^{1}A$_1$)												
ν_1(a$_1$)	147	154	145	131	107	114	104	100	94	99	92	87
ν_2(a$_1$)	278	288	287	260	187	197	198	155	141	146	111	113
ν_3(a$_1$)	302	309	331	307	241	247	249	237	224	231	216	205
ν_4(b$_1$)	i41	i38	93	48	29	29	40	24	21	14	46	35
ν_5(b$_2$)	182	191	278	217	147	156	156	133	113	122	124	91
ν_6(b$_2$)	233	242	442	345	173	180	194	152	194	202	193	170
C$_{2v}$-2(^{1}A$_1$)												
ν_1(a$_1$)	167	170	206	—^{a}	113	118	93	—^{a}	86	90	83	—^{a}
ν_2(a$_1$)	213	215	225		151	155	143		116	123	116	
ν_3(a$_1$)	385	391	412		305	311	304		259	265	282	
ν_4(b$_1$)	42	45	49		i29	i23	i1163		i68	i70	i23	
ν_5(b$_2$)	51	50	62		27	27	i22		i51	i49	85	
ν_6(b$_2$)	229	233	268		164	167	142		89	94	294	

^{a} It denotes the failure in the frequency calculation with the CCSD(T) method

2 s AO of Cl and can be viewed as lone pairs. Therefore, for three X$_3$Cl species only the remaining eight valence electrons need to be considered, which occupy four the highest MOs, denoted similarly HOMO and HOMO-n

(n=1-3) respectively. Valence MO pictures for all three cationic trigonal (D$_{3h}$) X$_3^+$ and three neutral trigon-pyramidal (C$_{3v}$) X$_3$Cl (X=Sc, Y, and La) isomers are drawn in Fig. 2 based on their optimized structures using

Table 4 The resonance energies (REs, in kcal mol^{-1}, corrected with ZPE) calculated with two schemes described in Sect. 2 for the regular trigonal X$_3^+$ (X=Sc, Y, and La) isomers

	Boldyrev's scheme				Dewar's scheme			
	X$_3$Cl (C$_{2v}$-1, ^{1}A$_1$)	X$_2$($^1\Sigma_g$)	XCl($^1\Sigma$)	RE$_1$	X$_3^+$ (D$_{3h}$, ^{1}A$'_1$)	X$_2$($^1\Sigma_g$)	X$^+$(^{1}S)	RE$_2$
Sc$_3^+$								
B3LYP	-2742.27377	-1521.24704	-1220.94406	51.9	-2281.71687	-1521.24704	-760.32231	92.6
MP2	-2738.99674	-1519.43084	-1219.46872	61.0	-2279.03237	-1519.43084	-759.45103	94.4
CCSD(T)	-2739.06051	-1519.45487	-1219.50054	66.0	-2279.08803	-1519.45487	-759.46257	107.0
Y$_3^+$								
B3LYP	-574.00496	-75.72316	-498.19108	56.9	-113.47401	-75.72316	-37.58640	103.2
MP2	-572.50579	-75.07934	-497.30894	73.7	-112.56048	-75.07934	-37.30724	109.1
CCSD(T)	-572.55628	-75.10087	-497.33761	73.9	-112.59940	-75.10087	-37.31847	113.0
La$_3^+$								
B3LYP	-553.90615	-62.35079	-491.47617	49.7	-93.35881	-62.35079	-30.91248	60.0
MP2	-552.42202	-61.73861	-490.60093	51.8	-92.45906	-61.73861	-30.60745	70.9
CCSD(T)	-552.46662	-61.75069	-490.63034	53.7	-92.50713	-61.75069	-30.62129	84.8

Table 5 Calculated NICS values (ppm cgsu) of the trigonal X_3^+, trigon-pyramidal X_3Cl (X=Sc, Y, La), and Mg_3Na^- species

Species	Methods	NICS(0.0)	NICS(0.5)	NICS(1.0)	NICS(1.5)
Sc_3^+					
(D_{3h}, $^1A'_1$)	HF	-28.47	-17.25	-4.20	0.81
	B3LYP	2738.36	1891.31	631.99	20.01
Sc_3Cl					
(C_{3v}, $^1A_1$)	HF	6.33	-11.68	-28.27	-63.11
	B3LYP	20.79	-6.40	-20.16	-45.26
Y_3^+					
(D_{3h}, $^1A'_1$)	HF	-25.10	-18.84	-9.02	-3.19
	B3LYP	-36.08	-25.79	-10.21	-2.04
Y_3Cl					
(C_{3v}, $^1A_1$)	HF	5.15	-10.05	-23.29	-52.95
	B3LYP	10.86	-13.39	-27.46	-50.22
La_3^+					
(D_{3h}, $^1A'_1$)	HF	-166.48	-126.03	-46.97	11.32
	B3LYP	-121.42	-104.12	-65.02	-28.32
La_3Cl					
(C_{3v}, $^1A_1$)	HF	29.52	5.25	-3.26	-23.74
	B3LYP	73.28	19.85	-10.84	-36.93
Mg_3Na^-					
(C_{3v}, $^1A_1$)	HF	-24.08	-24.06	-22.58	-19.96
	B3LYP	-22.58	-22.31	-20.69	-18.34

MP2 method and basis set 6-311 + G* for Sc, Cl atoms, basis set LANL2DZ for heavier Y, La atoms. The similar valence MO pictures of the monoanionic trigon-pyramidal (C_{3v}) Mg_3Na^- species based on the optimized structures with MP2/6-311 + G(d) are also drawn in Fig. 2 for comparison. Kuznetsov and Boldyrev showed that the monodianionic trigonal (D_{3h}) Mg_3^{2-} unit in Mg_3Na^- species has one π-delocalized HOMO ($2a_1$) and exhibits single π-aromaticity [32]. Here we prove through following MO analyzes that, analogous to Mg_3^{2-}, three cationic trigonal (D_{3h}) X_3^+ clusters possess only single π- or σ- aromaticity originating primarily from d AOs of the transition metal atoms Sc, Y, and La.

From Fig. 2 one can see that two HOMOs ($1a_2''$) for Sc_3^+, Y_3^+ are regarded as π-delocalized MOs, each resulting from the overlap of three out-of-plane d orbitals oriented radially toward the center of the trigon mainly composed of the d_{xz} and d_{yz} AOs of the corresponding component X atoms. The HOMO ($2a_1'$) for La_3^+, is regarded as σ-delocalized MOs, resulting from the overlap of three in-plane d orbitals oriented radially toward the center of the trigon mainly composed of the $d_{x^2-y^2}$ and d_{xy} AOs of La atoms. The remaining three valence MOs: the two-fold degenerate HOMO-1 ($1e'$), HOMO-2 ($1e'$), and HOMO-3 ($1a_1'$) for three X_3^+ cations are bonding-antibonding ($1e'$), nonbonding ($1e'$), and bonding ($1a_1'$) orbitals formed primarily from the filled valence s orbitals

with rather small contributions from d orbitals. The net bonding effect is expected to be close to zero and the s AOs can be viewed as lone pairs. Therefore, the number of valence π or σ electrons in the trigonal Sc_3^+, Y_3^+, and La_3^+ cations all conform to Hückel (4n + 2) rule for aromaticity respectively. The trigonal Sc_3^+ and Y_3^+ isomers exhibit single π-aromaticity and the trigonal La_3^+ isomer single σ-aromaticity. The bonding natures for these three cations are similar to that of the trigonal Mg_3^{2-} unit in Mg_3Na^- species (Fig. 2 and Ref. 32, Fig. 2). The main difference between X_3^+ and Mg_3^{2-} is that for X_3^+, the π or σ bonding MOs are composed of d AOs of the corresponding transition metal X atoms, whereas for Mg_3^{2-}, the π bonding MO is composed of p AOs of Mg atoms (Fig. 2, HOMO ($2a_1$) for Mg_3Na^-).

Figure 2 also shows that the two sets of MOs for La_3^+ (D_{3h}) and La_3Cl (C_{3v}) clusters are very similar although their MO orders are slightly varied. The MO pictures of the trigonal La_3^+ units in the neutral La_3Cl (C_{3v}) cluster is almost identical to the ones of the isolated La_3^+ isomer. Both have only one σ-type delocalized MO (Fig. 2, HOMO ($2a_1'$) for La_3^+ and HOMO-2 ($2a_1$) for La_3Cl (C_{3v})). For Sc_3^+, Y_3^+ and Sc_3Cl, Y_3Cl, Fig. 2 shows that the π-type MOs of Sc_3^+ and Y_3^+ are changed into the σ-type MOs (Fig. 2, HOMO-2 ($2a_1$) for Sc_3Cl, Y_3Cl) when the monoanionic counterions Cl^- is added to Sc_3^+, Y_3^+ cations respectively. Thus, for isolated Sc_3^+, Y_3^+, and La_3^+ cations
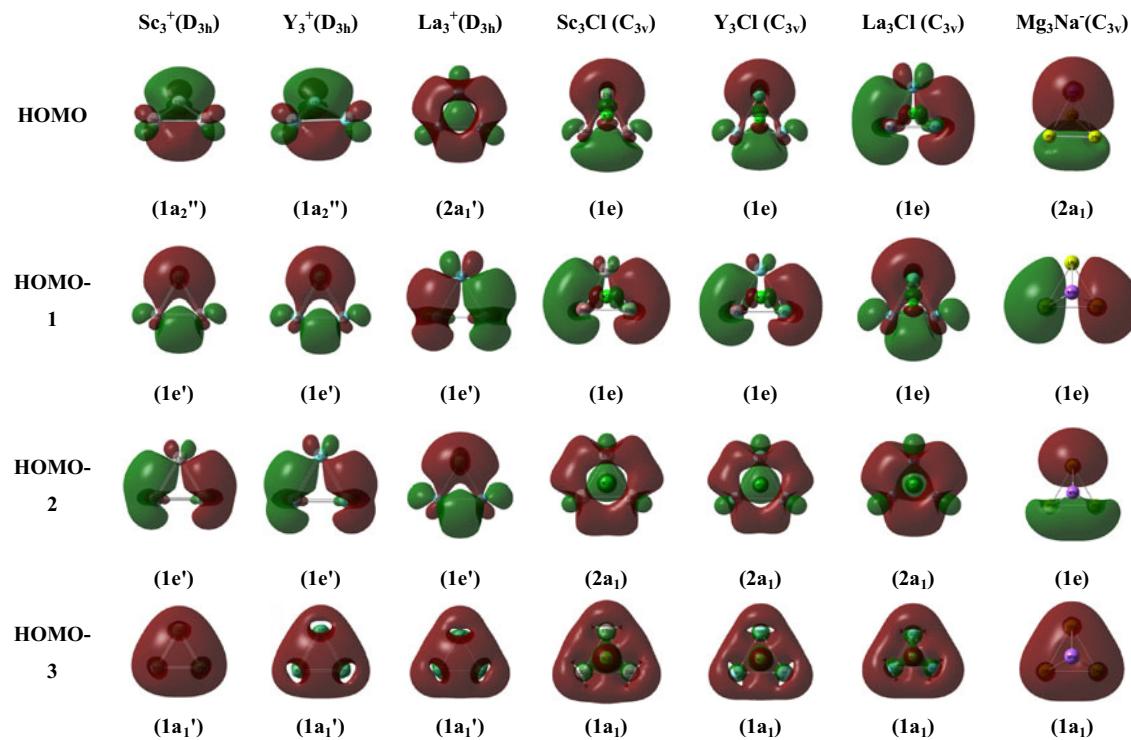
Fig. 2 Valence MO pictures for the trigonal X_3^+ (X = Sc, Y, La), the trigon-pyramidal X_3Cl (X = Sc, Y, La), as well as the trigon-pyramidal Mg_3Na^- clusters

there are two types of aromaticity: π-aromaticities for Sc_3^+, Y_3^+ and σ-aromaticity for La_3^+, but for Sc_3^+, Y_3^+, and La_3^+ units in corresponding X_3Cl (C_{3v}) clusters, they all are single σ-aromaticities. This case indicates that maybe addition of a counterion to some cluster can cause the change of aromatic type of this cluster.

Compared with the aromaticities of three anionic clusters X_3^- (X = Sc, Y, and La), which are corroborated to possess doublet σ and π aromatic characters [38]. Because the anionic clusters X_3^- (X = Sc, Y, and La) each has two value electrons more than the cationic X_3^+, it is reasonable that the former possess doublet aromaticity and the latter possess singlet.

Conclusions

The calculated results show that the X_3^+ cations each has two stable structures: the regular trigon (D_{3h}) and the line ($D_{\infty h}$) with the regular trigon (D_{3h}) being the ground state, while for three neutral X_3Cl clusters, Sc_3Cl has three stable isomers: the trigon-pyramidal (C_{3v}), bidentate (C_{2v}-1), and C_{2v}-2 structures, Y_3Cl and La_3Cl each has only two stable isomers: the trigon-pyramidal (C_{3v}) and bidentate (C_{2v}-1) structures. The ground states for three X_3Cl (X = Sc, Y, La) species are all the bidentate (C_{2v}-1) isomers. The calculations

of the REs and NICSs for the cationic trigonal X_3^+ isomers show that these trigonal X_3^+ isomers exhibit higher degree of aromaticity. The detailed molecular orbital analyzes reveal that the isolated trigonal Sc_3^+ and Y_3^+ cations has one delocalized π-type MO and shows single π-aromaticity, while the isolated trigonal La_3^+ cation has one delocalized σ-type MO and shows single σ-aromaticity. The single π- or σ-aromaticity for X_3^+ are mainly attributed to the contributions from the d AOs of the corresponding transition metal X atoms. However, when a singly negatively charged counterion Cl^- is added to Sc_3^+, Y_3^+, and La_3^+ cations respectively, the aromatic type for the two Sc_3^+, Y_3^+ units in the corresponding neutral Sc_3Cl, Y_3Cl complexes are changed from π-aromaticity into σ-aromaticity, whereas the σ-aromaticity of the La_3^+ units in the La_3Cl species keeps unchanged in this process. Thus three Sc_3^+, Y_3^+, La_3^+ units in the corresponding X_3Cl complexes all have only one σ-type MO and exhibit single σ-aromaticity.

References

1. Krygowski TM, Cyranski MK, Czarnocki Z, Häfelinger G, Katritzky AR (2000) Tetrahedron 56:1783–1796

2. Minkin VI, Glukhovstev MN, Simkin BY (1994) Aromaticity and antiaromaticity: electronic and structural aspect. Wiley, New York
3. Li X, Kuznetsov AE, Zhang HF, Boldyrev AI, Wang LS (2001) Observation of all-metal aromatic molecules. Sci 291:859–861
4. Li X, Zhang HF, Wang LS, Kuznetsov AE et al. (2001) Experimental and theoretical observations of aromaticity in heterocyclic XAl3- (X = Si, Ge, Sn, Pb) systems. Angew Chem Int Ed 40:1867–1870
5. Kuznetsov AE, Boldyrev AI, Li X et al. (2001) On the aromaticity of square planar Ga_4^{2-} and In_4^{2-} in Gaseous $NaGa_4^-$ and $NaIn_4^-$ clusters. J Am Chem Soc 123(36):8825–8831
6. Boldyrev AI, Kuznetsov AE (2002) On the resonance energy in new all-metal aromatic molecules. Inorg Chem 41(3):532–537
7. Kuznetsov AE, Boldyrev AI, Zhai HJ et al. (2002) Al62- − fusion of two aromatic Al3- units. a combined photoelectron spectroscopy and ab initio study of M + [Al62-] (M = Li, Na, K, Cu, and Au). J Am Chem Soc 124(39):11791–11801
8. Kuznetsov AE, Boldyrev AI (2002) Theoretical evidence of aromaticity in X_3^- (X = B, Al, Ga) Species. Struct Chem 13 (2):141–148
9. Alexandrova AN, Boldyrev AI (2003) σ-aromaticity and σ-antiaromaticity in alkali metal and alkaline earth metal small clusters. J Phys Chem A 107(4):554–560
10. Tanaka H, Neukermans S, Janssens E et al. (2003) σ aromaticity of the bimetallic Au_5Zn^+ cluster. J Am Chem Soc 125(10):2862–2863
11. Chi XX, Li XH, Chen XJ, Yuang ZS (2004) Ab initio studies on the aromaticity of bimetallic anionic clusters XGa3- (X=Si, Ge). J Mol Struct THEOCHEM 677:21–27
12. Lin YC, Sundholm D, Jusélius J et al. (2006) Experimental and computational studies of alkali-metal coinage-metal clusters. J Phys Chem A 110(12):4244–4250
13. Boldyrev AI, Wang LS (2005) All-metal aromaticity and antiaromaticity. Chem Rev 105(10):3716–3757
14. Bühl M, Hirsch A (2001) Spherical aromaticity of fullerenes. Chem Rev 101(5):1153–1184
15. Cui LF, Huang X, Wang LM et al. (2006) Sn_{12}^{2-}: stannaspherene. J Am Chem Soc 128(26):8390–8391
16. Cui LF, Huang X, Wang LM et al. (2006) Pb_{12}^{2-}: plumbaspherene. J Phys Chem A 110(34):10169–10172
17. Sun ZM, Xiao H, Li J et al. (2007) $Pd_2@Sn_{18}^{4-}$: fusion of two endohedral stannaspherenes. J Am Chem Soc 129(31):9560–9561
18. Neukermans S, Janssens E, Chen Zf et al. (2004) Extremely stable metal-encapsulated $AlPb_{10}^+$ and $AlPb_{12}^+$ clusters: mass-spectrometric discovery and density functional theory study. Phys Rev Lett 92(6):163401-1–163401-4
19. Chen ZF, Neukermans S, Wang X et al. (2006) To achieve stable spherical clusters: general principles and experimental confirmations. J Am Chem Soc 128(39):12829–12834
20. Chen Z, King RB (2005) Spherical aromaticity: Recent work on fullerenes, polyhedral boranes, and related structures. Chem Rev 105(10):3613–3642
21. Proft FD, Geerlings P (2001) Conceptual and computational DFT in the study of aromaticity. Chem Rev 101(5):1451–1464
22. Jiao HJ, PvR S, Mo Y et al. (1997) Magnetic evidence for the aromaticity and antiaromaticity of charged fluorenyl, indenyl, and cyclopentadienyl systems. J Am Chem Soc 119(30):7075–7083
23. Quiñonero D, Frontera A, Ballester P et al. (2000) A theoretical study of aromaticity in squaramide and oxocarbons. Tetrahedron Lett 41:2001–2005
24. Jemmis ED, Kiran B (1998) Aromaticity in X3Y3H6 (X = B, Al, Ga; Y = N, P, As), X3Z3H3 (Z = O, S, Se), and phosphazenes.

Theoretical study of the structures, energetics, and magnetic properties. Inorg Chem 37(9):2110–2116
25. Schleyer PvR, Maerker C, Dransfeld A et al. (1996) Nucleus-independent chemical shifts: a simple and efficient aromaticity probe. J Am Chem Soc 118(26):6317–6318
26. PvR S, Jiao H, NJRvE H et al. (1997) An evaluation of the aromaticity of inorganic ring: refined evidence from magnetic properties. J Am Chem Soc 119(51):12669–12670
27. PvR S, Manoharan M, Wang ZX et al. (2001) Dissected nucleus-independent chemical shift analysis of π-aromaticity and antiaromaticity. Org Lett 3(16):2465–2468
28. Kirchner B, Sebastiani D (2004) Visualizing degrees of aromaticity for different barbaralane systems. J Phys Chem A 108 (52):11728–11732
29. Sirockin F, Dejaegere A (2005) Magnetic effects of disulfide bridges: a density functional and semiempirical study. J Phys Chem B 109(8):3627–3638
30. Li QS, Cheng LP (2003) Aromaticity of square planar N_4^{2-} in the M_2N_4 (M = Li, Na, K, Rb, or Cs) species. J Phys Chem A 107 (16):2882–2889
31. Zhan CG, Zheng F, Dixon DA (2002) Electron affinities of Aln clusters and multiple-fold aromaticity of the square Al_4^{2-} structure. J Am Chem Soc 124(49):14795–14803
32. Kuznetsov AE, Boldyrev AI (2004) A single π-bond captures 3, 4 and 5 atoms. Chem Phys Lett 388:452–456
33. Tsipis AC, Tsipis CA (2003) Hydrometal analogues of aromatic hydrocarbons: a new class of cyclic hydrocoppers (I). J Am Chem Soc 125(5):1136–1137
34. Huang X, Zhai HJ, Kiran B et al. (2005) Observation of d-orbital aromaticity. Angew Chem Int Ed 44:7251–7254
35. Wannere CS, Corminboeuf C, Wang ZX et al. (2005) Evidence for d orbital aromaticity in square planar coinage metal clusters. J Am Chem Soc 127(15):5701–5705
36. Alexandrova AN, Boldyrev AI, Zhai HJ et al. (2005) $Cu_3C_4^-$: A new sandwich molecule with two revolving C_2^{2-} units. J Phys Chem A 109(4):562–570
37. Liu Y, Wu SD, Chi XX (2007) Theoretical study of aromaticity in small hydrogen and metal cation clusters X_3^+ (X = H, Li, Na, K, and Cu). Int J Quant Chem 107(3):722–728
38. Chi XX, Liu Y (2007) Theoretical evidence of d-orbital aromaticity in anionic metal X_3^- (X = Sc, Y, La) clusters. Int J Quant Chem 107 (9):1886–1896
39. Becke AD (1993) Density-functional thermochemistry. III. The role of exact exchange. J Chem Phys 98(7):5648–5652
40. Lee C, Yang W, Parr RG (1988) Development of the colle-salvetti correlation-energy formula into a functional of the electron density. Phys Rev B 37(2):785–789
41. Perdew JP, Wang Y (1992) Accurate and simple analytic representation of the electron-gas correlation energy. Phys Rev B 45(23):13244–13249
42. Møller C, Plesset MS (1934) Note on an approximation treatment for many-electron systems. Phys Rev 46:618–622
43. Head-Gordon M, Pople JA, Frisch MJ (1988) MP2 energy evaluation by direct methods. Chem Phys Lett 153(6):503–506
44. Cizek J (1969) On the use of the cluster expansion and the technique of diagrams in calculations of correlation effects in atoms and molecules. Adv Chem Phys 14:35–89
45. Purvis GD III, Bartlett RJ (1982) A full coupled-cluster singles and doubles model: the inclusion of disconnected triples. J Chem Phys 76:1910–1918
46. Scuseria GE, Janssen CL, Schaefer HF III (1988) An efficient reformulation of the closed-shell coupled cluster single and double excitation (CCSD) equations. J Chem Phys 89:7382–7387

47. Pauling L (1960) The nature of the chemical bond and structureof molecules in crystals, 3rd edn. Cornell University Press, Ithaca
48. Pauling L, Wheland GW (1933) The nature of the chemical bond. V. The quantum-mechanical calculation of the resonance energy of benzene and naphthalene and the hydrocarbon free radicals. J Chem Phys 1:362–374
49. Wheland GW (1955) Resonance in organic chemistry. Wiley, New York
50. Pauling L, Sherman J (1933) The nature of the chemical bond.VI. The calculation from thermochemical data of the energy of resonance of molecules among several electronic structures. J Chem Phys 1:606–617
51. Dewar MJS, DeLlano C (1969) Ground states of conjugated molecules. XI. Improved treatment of hydrocarbons. J Am Chem Soc 91(4):789–795
52. Williams RV (2001) Homoaromaticity. Chem Rev 101(5):1185–1204
53. Tsipis CA (2005) DFT study of "all-metal" aromatic compounds. Coord Chem Rev 249:2740–2762
54. Frisch MJ, Trucks GW, Schlegel HB, Scuseria GE, Robb MA, Cheeseman JR et al. (2003) Gaussian03, Revision C.02. Gaussian Inc, Wallingford
55. Frisch Æ, DenningtonII RD, Keith TA et al. (2003) Gaussview03. Gaussian Inc, Wallingford